【 CASE REPORT 】

Cancer-associated Retinopathy with Neuroendocrine Combined Large-cell Lung Carcinoma and Adenocarcinoma

Kyoko Yagyu [1], Takahiro Ueda [1], Atsushi Miyamoto [1], Riki Uenishi [1], Haruhiko Matsushita [1] and Tomonori Tanaka [2]

Abstract:

We herein report the case of a 74-year-old woman with a lung tumor. She presented with complaints of blurred and rapid, progressively impaired vision. A visual field examination revealed bilateral concentric contraction of the visual field and a ring scotoma in the right eye. She was diagnosed with cancer-associated retinopathy (CAR) combined with large-cell neuroendocrine carcinoma (LCNEC) of the lung via a visual field examination and underwent thoracoscopic surgery. CAR has been mostly associated with small-cell lung cancer (SCLC). Combined LCNEC is relatively rare and accounts for 10.6% of all LCNECs. This is the first case report of CAR-combined LCNEC.

Key words: cancer-associated retinopathy, combined large-cell neuroendocrine carcinoma, vision impairment

(Intern Med 58: 3289-3294, 2019)
(DOI: 10.2169/internalmedicine.2313-18)

Introduction

Cancer-associated retinopathy (CAR) is a paraneoplastic neurological syndrome characterized by retinal degeneration. It is an acquired retinochoroidal degeneration disorder that develops clinical symptoms resembling retinal pigmentary degeneration. The manifestation of retinopathy might aid in early cancer detection, as it can develop before the primary lesion is clinically discovered (1, 2). The majority of CAR-associated solid tumors are small-cell lung cancers (SCLCs), followed by digestive and gynecological system cancers (3, 4). Only three cases of CAR-complicated large-cell lung carcinoma (LCLC) have been reported to date (5-7).

We herein report for the first time a case of CAR-complicated large-cell neuroendocrine carcinoma (LCNEC) and adenocarcinoma.

Case Report

A 74-year-old woman complained of blurred vision starting from October 2015. She underwent bilateral cataract surgery at an ophthalmological clinic in March 2016; however, she was dissatisfied with her postoperative misty vision. Vision loss was identified during visual acuity testing. Rapid progression of vision loss indicated the possibility of CAR.

Chest X-ray performed during a referral visit to our hospital at the beginning of May revealed a mass shadow in the left lower lung field (Fig. 1a). Chest computed tomography (CT) revealed a nodule (diameter, roughly 17 mm) under the pulmonary pleura in the left lower lobe (S^{10}) and lymphadenopathy in the left lung hilum (Fig. 1b). Her smoking history was 20 cigarettes per day for 52 years. The patient did not have a family history of retinal disorders. An ophthalmologic examination revealed anterior chamber cells and vitreous opacities. The best-corrected visual acuity of the right eye was 4/20, and that of the left eye was 3/20, revealing progressive loss of vision. The intraocular pressures of the right and left eyes were 16 and 15 mmHg, respectively. The patient showed no other ophthalmological or neurological symptoms. Magnetic resonance imaging of the head revealed no abnormal retrobulbar lesions, and the intraorbital structures appeared normal. There was no abnormality in the eye fundus. A visual field examination revealed a bilateral concentric visual field with a narrowed visual field and a ring scotoma in the right eye (Fig. 2a). Dark-adapted Flash
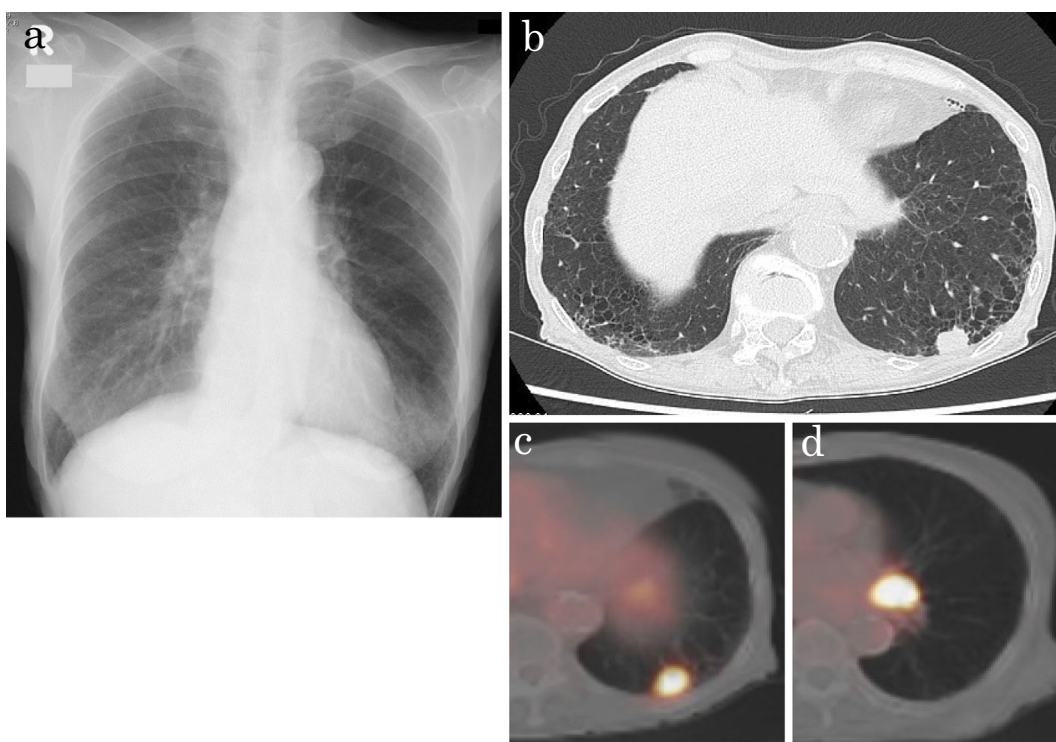
Figure 1. (a) Chest X-ray showing a mass shadow at the left lower lung field. (b) Chest CT scan showing a nodule with notching and spicula formation under the pleural cavity in the left lower lobe and lymphadenopathy in the left hilum of the lung. (c) Whole-body positron emission tomography showing the lung lesion, with an SUV$_{max}$ of 11.6 for the nodule in the left lower lobe. (d) Whole-body positron emission tomography showing the lymph node with an SUV$_{max}$ of 18.4 in the left hilum of the lung. CT: computed tomography, SUV: standardized uptake value

electroretinography of both eyes showed that the amplitudes of the a- and b-waves were practically extinguished (Fig. 2b). Photopic Flicker ERG of both eyes revealed markedly reduced responses (Fig. 2c).

Although the anti-recoverin antibody, which is widely recognized as an anti-retinal antibody, is positive in CAR patients, a Western blot analysis for recoverin [Recombx CAR (Anti-Recoverin) Autoantibody Test, Marlborough, USA] showed negative results (titer <50) after being performed twice in this patient. The pro-gastrin-releasing peptide (ProGRP) level was 130 ng/mL, and the levels of other tumor markers were within normal ranges. Furthermore, rheumatoid factor and antinuclear antibody tests were negative. The levels of IgG, IgA, and IgM immunoglobulins were 1,533 mg/dL, 335 mg/dL, and 174 mg/dL, respectively. The serum protein fraction revealed the expression of Alb (62.2%), α$_1$ (2.3%), α$_2$ (7.1%), β (8.7%), and γ (19.3%). These results eliminated the possibility of an autoimmune disease.

Although bronchoscopy was performed on the lower left lobe nodule, a definitive diagnosis could not be obtained. Whole-body positron emission tomography revealed an increased uptake of ^{18}F-fluorodeoxyglucose in the lung lesion, with a maximum standardized uptake value (SUV$_{max}$) of 11.6 (Fig. 1c). The SUV$_{max}$ in the left hilar lymph node was 18.4 (Fig. 1d). The clinical stage was T1bN1M0, stage IIB ac-

cording to the 8th edition of the tumor, node, metastasis (TNM) classification of the International Union Against Cancer (8). The patient underwent thoracoscopic partial resection of the left S^{10}. A pathological examination revealed a 22-mm tumor that had invaded beyond the elastic layer of the pleura (PL1). The pathological stage was T2aN1M0, stage IIB. The tumor consisted of two components with LCNEC and adenocarcinoma (Fig. 3a). A pathological specimen showed the tumor cell composition to be 90% LCNEC and 10% adenocarcinoma. The LCNEC had relatively large, atypical cells arranged in trabecular, rosette-like structures and solid sheets. These LCNEC cells were larger than the cells observed in small-cell carcinoma, which are characterized by eosinophilic cytoplasm and variably coarse chromatin (Fig. 3b). The adenocarcinoma showed glandular and papillary formation with mucus production and had abundant cytoplasm with nuclear polarity along the basement membrane (Fig. 3b). In addition, the LCNEC cells showed high mitotic activity (≥11 mitoses per 10 high-power fields) (Fig. 3b) and a high Ki67/MIB-1 index of 93% (Fig. 3c). Immunohistochemistry revealed positive nuclear expression of TTF1 in the adenocarcinoma component, but not in the LCNEC (Fig. 3d). The LCNEC component was positive for the neuroendocrine markers chromogranin A and synaptophysin (Fig. 3e and f). The final diagnosis based on the sudden visual disturbance and pathological
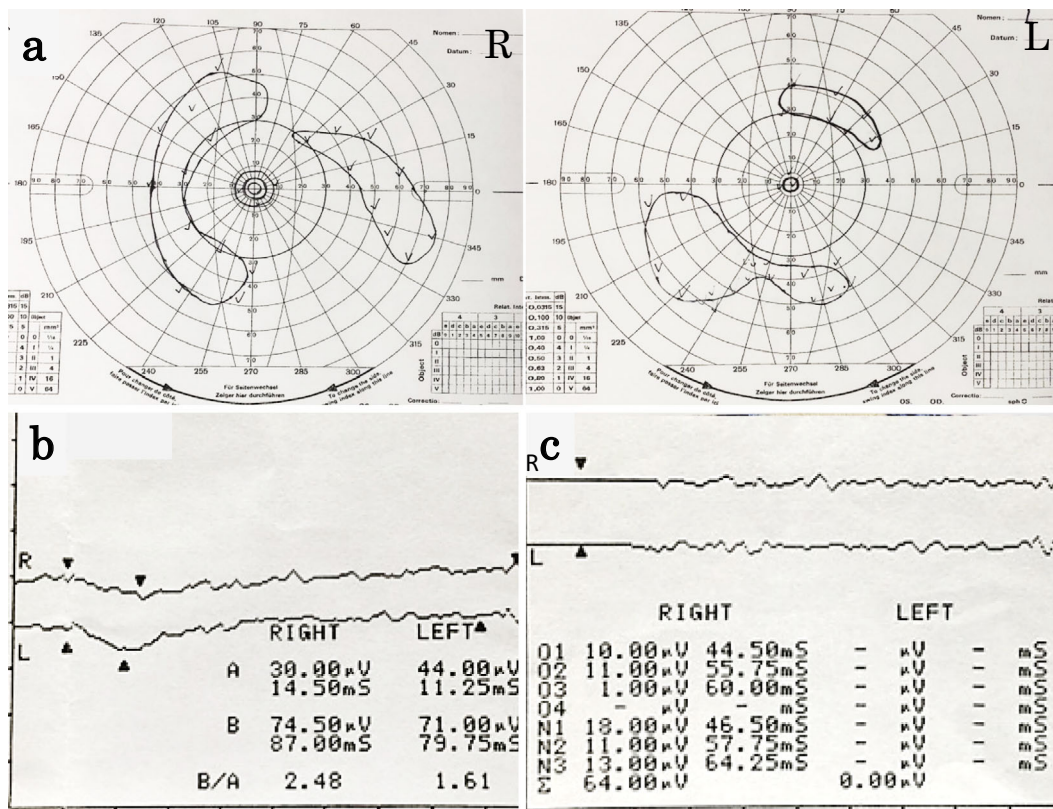
Figure 2. (a) Goldman visual field testing showing generalized field loss in both eyes and a ring scotoma in the right eye. (b) Dark-adapted Flash ERG of both eyes showing that the amplitudes of the a- and b-waves had been extinguished. (c) Photopic flicker ERGs of both eyes showing reduced responses. ERG: electroretinography

findings was CAR with combined neuroendocrine LCLC and adenocarcinoma.

Two weeks after the diagnosis, the patient received chemoradiotherapy (cisplatin+etoposide) because of lympho-vascular invasion. The patient underwent concurrent radiotherapy targeting the left hilar and mediastinal lymph nodes (60 Gy/30 fr) in mid-June. Prior to chemoradiotherapy, her left vision became limited to hand motion before the eyes despite treatment with oral steroids (prednisolone, 30 mg/day for 14 days). However, after two cycles of chemotherapy, her best-corrected visual acuity of the right eye was 20/16, and that of the left eye was 20/25, indicating recovery (Fig. 4). Follow-up chest CT after 3 cycles of chemotherapy revealed a >30% reduction in the size of the left hilar lymph node. Furthermore, the serum ProGRP level had decreased to 79 ng/mL, indicating a good partial response. In addition, the inflammation in the anterior segment of the eye disappeared. A visual field examination showed an improved visual field in August 2016 (Fig. 5). For 22 months after chemoradiotherapy initiation, the patient did not relapse, and her visual function remained stable. However, the patient developed lung metastases in the left upper lung field in March 2018. The patient requested best supportive care and achieved an overall survival of 27 months.

Discussion

CAR is a paraneoplastic neurological syndrome characterized by retinal degeneration, as first reported by Sawyer et al. in 1976 (1). As of 2001, approximately 100 CAR cases had been reported in the literature (9). CAR has been increasingly frequently recognized, and most recent searches turned up 90 CAR cases, including conference presentations and original papers, in Japan.

Lung cancer accounts for 40% of the cancers associated with CAR. Approximately 80% of all lung cancers are SCLCs, consistent with Adamus's description in 2009 (4). The majority of reports are focused on ophthalmologic examinations and lack a detailed description of the tumor pathology. To date, there have been three case reports of CAR-complicated LCNEC. In those cases, the diagnoses were confirmed from a pathological specimen of lymph node tissue obtained via mediastinoscopy (5), tissue from thickening pleura (undisclosed sampling method) (6), and a cytological specimen obtained via bronchofiberscopy (7). Given that LCNEC is a relatively rare disease, its clinical features are not well defined. A precise diagnosis requires a careful pathological examination owing to the high possibility of incorrectly diagnosing LCNEC as a poorly differentiated NSCLC or SCLC. The diagnosis of LCNEC from small bi-
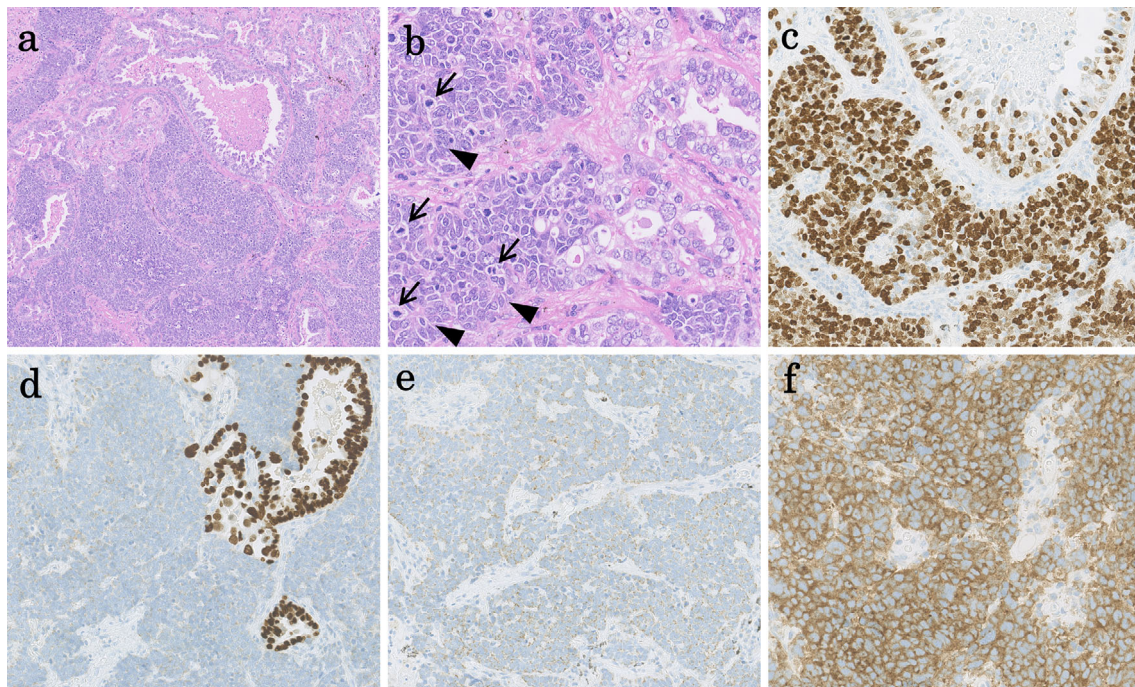
Figure 3. (a) Hematoxylin and Eosin staining, original, 4×. Low magnification shows the proliferation of tumor cells with an acinar pattern of adenocarcinoma (right upper) as well as a solid pattern of LCNEC (lower). A pathological examination revealed that the combined LCNEC and adenocarcinoma consisted of 90% LCNEC and 10% adenocarcinoma. (b) Hematoxylin and Eosin staining, original, 40×. On higher magnification, the adenocarcinoma(right) shows gland formation with a small amount of mucous production. The LCNEC(left) shows a solid nest with rosette-like structures (arrowheads) and nuclear moldings. The LCNEC cells shows relatively large nuclei with conspicuous mitoses (arrows). (c) Original, 20×. The LCNEC (lower) shows a Ki67/MIB-1 index of 93%, which is higher than that of adenocarcinoma (right upper). (d) Original, 20×. The adenocarcinoma component (right) shows positivity for TTF1, whereas the LCNEC component shows negativity. (e, f) Original, 20×. The neuroendocrine markers of chromogranin A (e) and synaptophysin (f) are positive in the LCNEC area. LCNEC: large-cell neuroendocrine carcinoma
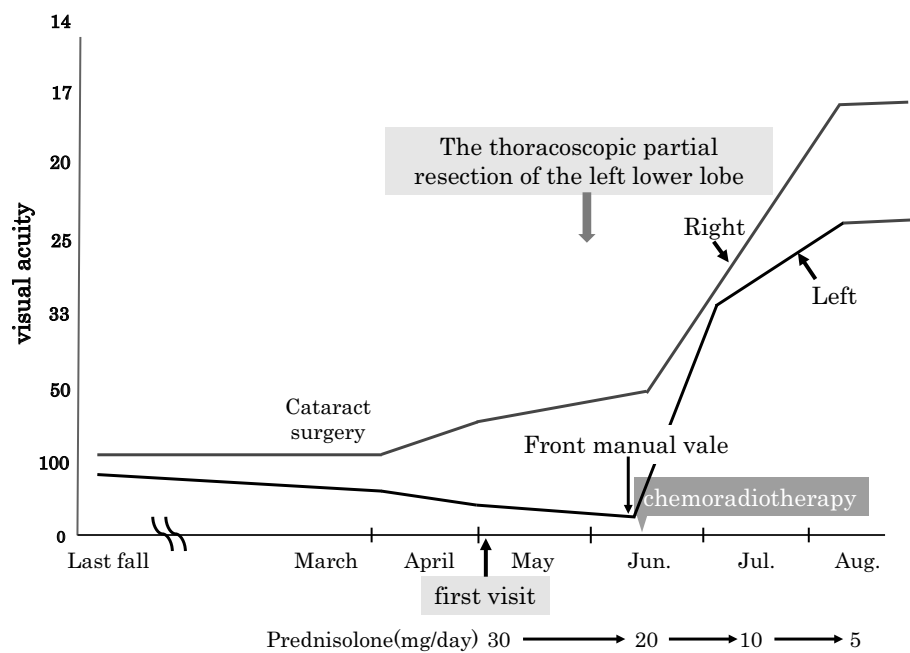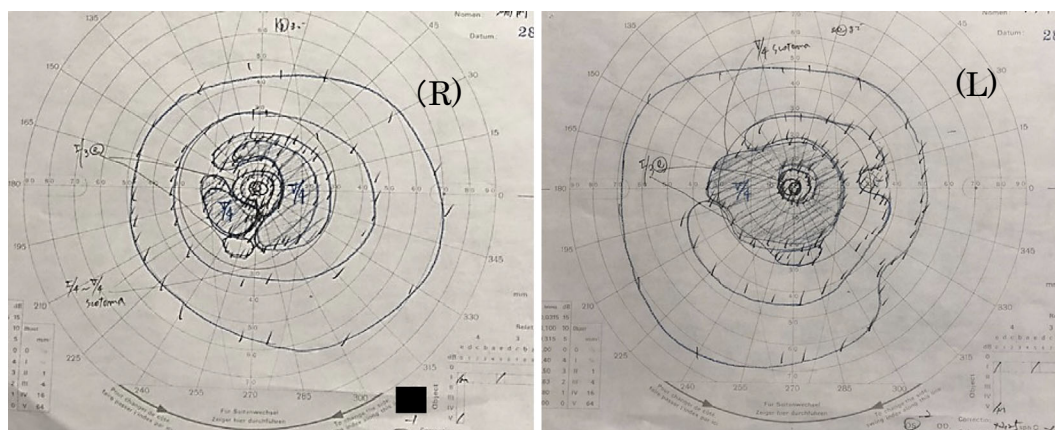

Figure 4. Clinical course.

Figure 5. **Goldman visual field testing showing improvement after chemoradiotherapy.**

opsies or cytological samples is also challenging (10). In fact, pulmonary LCNECs are rare tumors of the lung identified in a series of surgically resected specimens and account for only approximately 2-3% of all lung cancers (11). In addition, there are few case reports of CAR-complicated lung adenocarcinoma in the literature. The present case involved adenocarcinoma that was positive for the neuroendocrine marker CD56. It is thus a rare case of CAR-complicated LCNEC and adenocarcinoma diagnosed based on a surgically resected specimen.

The genetic characteristics of LCNECs are reportedly similar to those of SCLCs. A loss of heterozygosity analysis using microsatellite markers for the investigation of LCNEC, SCLC, and LCLC revealed deletions of 3p, 5q21, and 9p21, as well as loss of the hetero-bonding of retinoblastoma gene in both LCNEC and SCLC (12). Given that LCNEC and SCLC are classified as high-grade neuroendocrine tumors (13), they may be prone to causing paraneoplastic neuropathy in a single entity (14).

CAR is heterotopic and associated with the expression of an antibody against the retinal cell antigens that are aberrantly produced by cancer cells. An antigen commonly expressed in both tumor cells and retina causes retinal cellular injury and death via autoimmunity. Many such antibodies have been discovered, including the most widely recognized anti-recoverin, which is a highly immunogenic protein belonging to the neuron calcium sensor protein family (1, 15, 16). It is intrinsically expressed only on retinal visual cells, neurons, or neuroendocrine cells (17). However, recoverin antibody was negative in our patient.

There are no set diagnostic criteria for CAR, and it is generally diagnosed via sudden-onset visual dysfunctions and pathological examinations. It has been reported that anti-recoverin antibodies can only be detected in approximately 10% of patients with CAR (4). Furthermore, the detection of anti-retinal antibodies alone does not confirm a CAR diagnosis, as anti-recoverin antibodies can be found in the normal population and in patients with non-paraneoplastic autoimmune retinopathy (18).

At present, there is no established treatment protocol for CAR. The most widely reported treatment is steroid administration. However, this treatment has only been temporarily effective. In the present case, resection of the lung tumor and chemoradiotherapy improved the visual function, and the patient was stable for 22 months. The confirmation of a diagnosis before destruction of the retinal tissue might render CAR treatment more effective.

Informed consent for the publication of this report was obtained from the patient.

References

1. Sawyer RA, Shelhorst JB, Zimmerman LE, Hoyt WF. Blindness caused by photoreceptor degeneration as a remote effect of cancer. Am J Ophthalmol 81: 606-613, 1976.
2. Darnell RB, Posner JB. Paraneoplastic syndromes involving the nervous system. N Engl J Med 349: 1543-1554, 2003.
3. Misiuk-Hojo M, Jurowska-Liput J, Gorczyca W. Cancer associated retinopathy. Oncology 54: 584-586, 2004.
4. Adamus G. Autoantibody targets and their cancer relationship in the pathogenicity of paraneoplastic retinopathy. Autoimmun Rev 8: 410-414, 2009.
5. Stanford MR, Edelsten CE, Hughes JD, et al. Paraneoplastic retinopathy in association with large cell neuroendocrine bronchial carcinoma. Br J Ophthalmol 79: 617-618, 1995.
6. Nakamura T, Fujisaka Y, Tamura Y, et al. Neuroendocrine carcinoma of the lung with cancer-associated retinopathy. Large Cell Case Rep Oncol 8: 153-158, 2015.
7. Isaka M, Kubota T, Sakai M, Yamane T, Ohnishi H, Yokoyama A. Cancer-associated retinopathy in a patient with large-cell neuroendocrine carcinoma of the lung. Nihon Kokyuuki Gakkaishi (Ann Jpn Respir Soc) 2: 39-43, 2013 (in Japanese, Abstract in English).
8. The Japan Lung Cancer Society. General Rule for Clinical and Pathological Record of Lung Cancer. 8th ed. Kanehara, Tokyo,

2017: 3-11 (in Japanese).

9. Arnold AC, Lee AG. Systemic disease and neuro-ophthalmology: annual update 2000. J Neuroophthalmol **21**: 46-61, 2001.

10. Fasano M, Corte CMD, Papaccio F, Ciardiello F, Morgillo F. Pulmonary large-cell neuroendocrine carcinoma from epidemiology to therapy. J Thorac Oncol **10**: 1133-1141, 2015.

11. Iyoda A, Hiroshima K, Toyozaki T, et al. Clinical characterization of pulmonary large cell neuroendocrine carcinoma and large cell carcinoma with neuroendocrine morphology. Cancer **91**: 1992-2000, 2001.

12. Hiroshima K, Iyoda A, Shibuya K, et al. Genetic alterations in early-stage pulmonary large cell neuroendocrine carcinoma. Cancer **100**: 1190-1198, 2004.

13. Naranjo Gómez JM, Gómez Román JJ. Behaviour and survival of high-grade neuroendocrine carcinomas of the lung. Respir Med **104**: 1929-1936, 2010.

14. Zhao X, McCutcheone JN, Kallakury B, et al. Combined small cell carcinoma of the lung: is it a single entity? J Thorac Oncol **13**: 237-245, 2018.

15. Polans AS, Buczylko J, Crabb J, Palczewski K. A photoreceptor calcium binding protein is recognized by autoantibodies obtained from patients with cancer-associated retinopathy. J Cell Biol **112**: 981-989, 1991.

16. Adamus G, Ren G, Weleber RG. Autoantibodies against retinal proteins in paraneoplastic and autoimmune retinopathy. BMC Ophthalmology **4**: 5, 2004.

17. Kawamura S. Rhodopsin phosphodiesterase regulation by S-modulin. Nature **362**: 855-857, 1991.

18. Shimazaki K, Jirawuthiworavong GV, Heckenlively JR, Gordon LK. Frequency of anti-retinal antibodies in normal human serum. J Neuro-Ophthalmol **28**: 5-11, 2008.